

**Structural and mechanistic insight into Holliday junction dissolution by  
Topoisomerase III $\alpha$  and RMI1**

Nicolas Bocquet<sup>1</sup>, Anna H. Bizard<sup>2</sup>, Wassim Abdulrahman<sup>1</sup>, Nicolai B. Larsen<sup>2</sup>,  
Mahamadou Faty<sup>1</sup>, Simone Cavadini<sup>1</sup>, Richard D. Bunker<sup>1</sup>, Stephen C.  
Kowalczykowski<sup>3</sup>, Petr Cejka<sup>3,4</sup>, Ian D. Hickson<sup>2</sup> & Nicolas H. Thomä<sup>1</sup>.



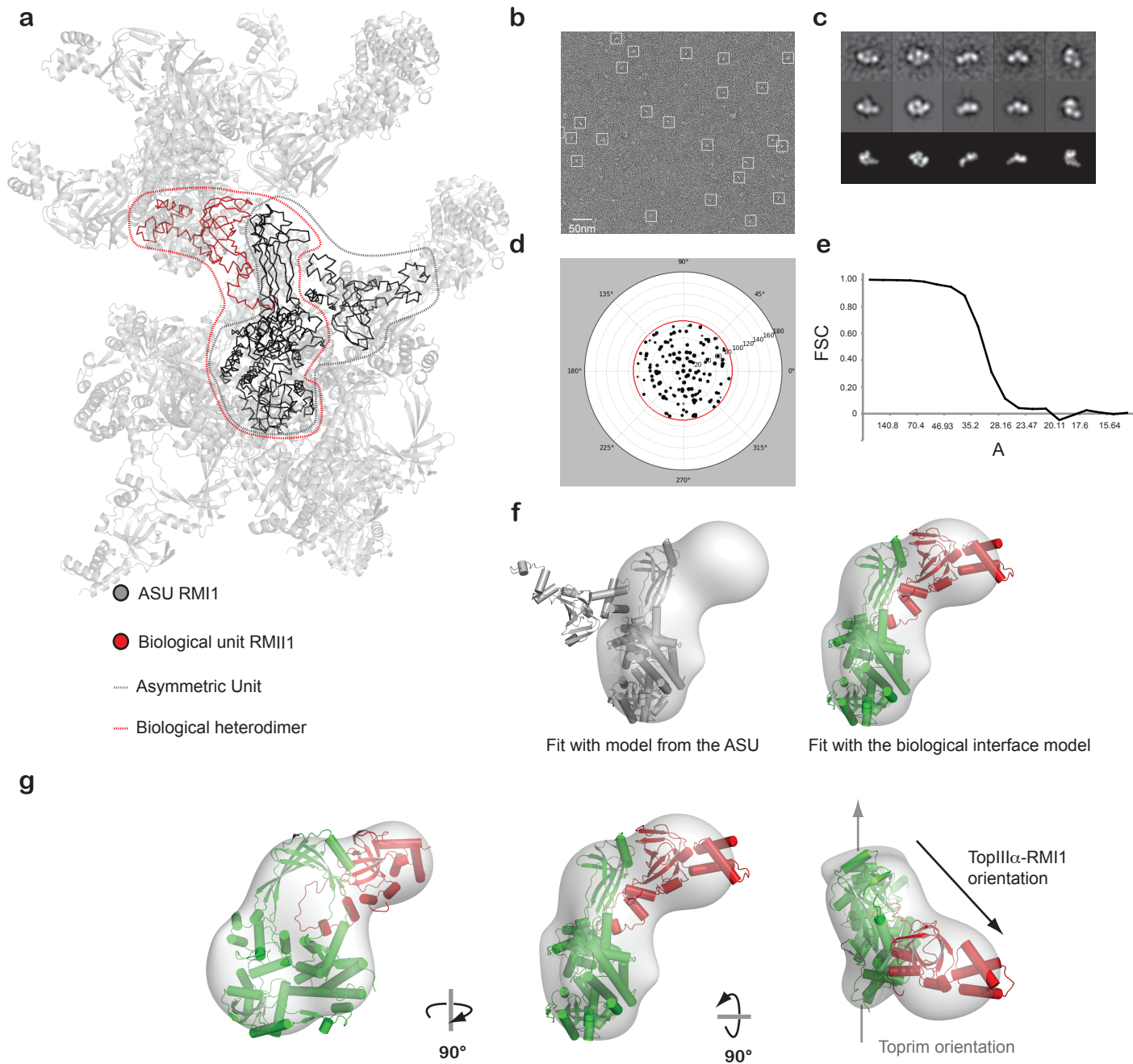
### Supplementary figure 1

**Topoisomerases alignment.** Human TopIII $\alpha$  is the upper sequence; 2. *Saccharomyces cerevisiae* Top3; 3. *Escherichia coli* Top3; 4. *Escherichia coli* Top1A; 5. *Thermatoga maritima* Top1A. The alignment has been made with T-COFFEE (<http://tcoffee.vital-it.ch>) and edited to show similarity percentage with a threshold set up at 3. Percentage of similarity is coloured as a gray scale, the four different levels being (from white to black): White is less than 60%, light gray is between 60 to 80%, dark gray is 80 to 99% and black is 100%.



## Supplementary figure 2

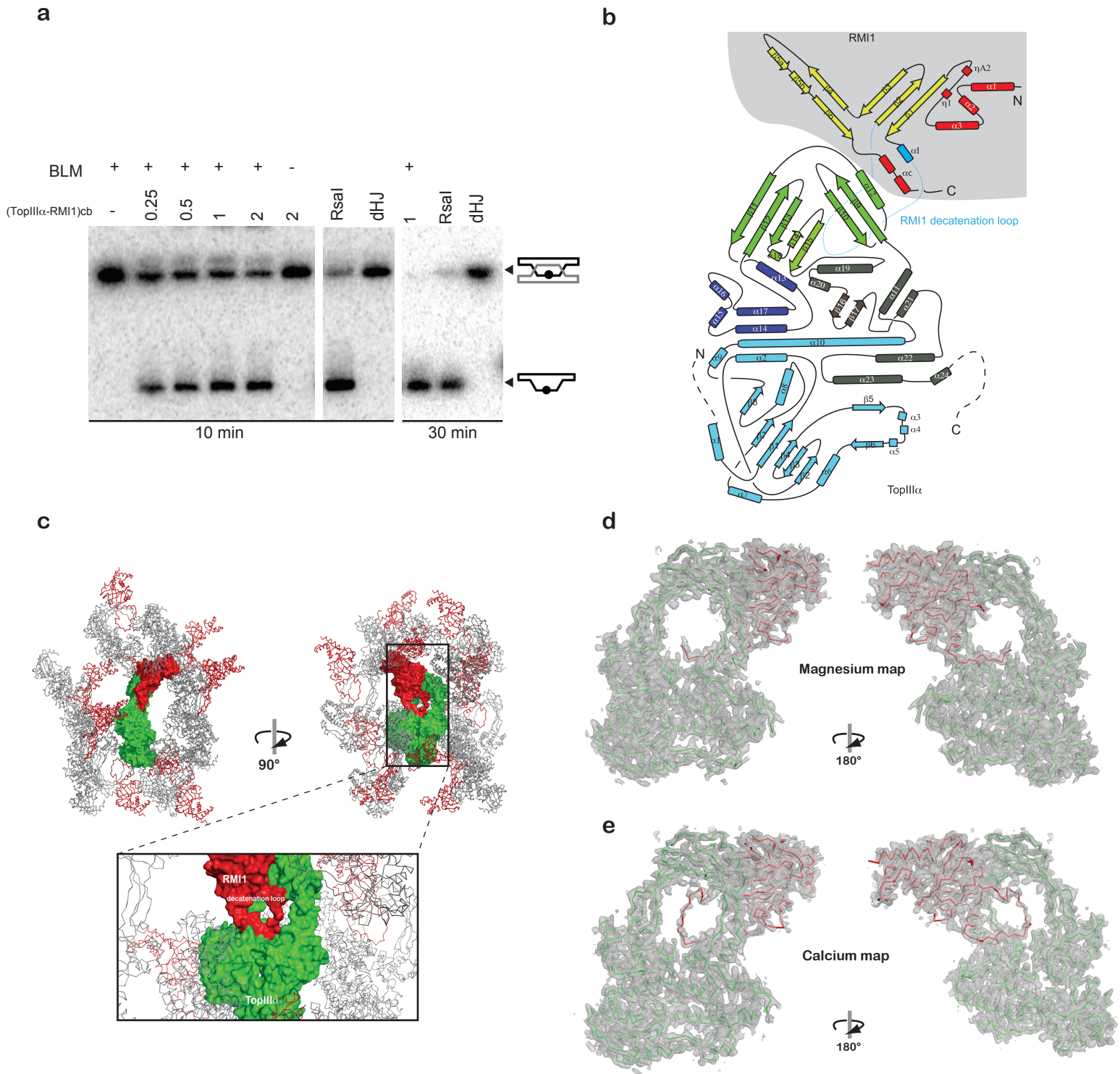
**Overall conservation.** Percentage of conservation projected on the TopIII $\alpha$ -RMI1 complex. Topoisomerase conservation has been calculated from the sequences in Supplementary fig.2 and RMI1 conservation from the sequences in panel b. b) RMI1 comparison between human RMI1 and several yeast Rmi1. 1. *Saccharomyces cerevisiae*; 2. *Zygosaccharomyces rouxii*; 3. *Pichia pastoris*; 4. *Schizosaccharomyces japonicus*; 5. *Grossmannia clavigera*; 6. *Colletotrichum graminicola*; 7. *Colletotrichum higginsanum*; 8. *Candida dubliniensis*; 9. *Schizosaccharomyces pombe*; 10. *Homo sapiens*



Supplementary fig. 3

### Supplementary figure 3

**Biological heterodimer vs asymmetric unit heterodimer.** a) A crystal packing diagram showing the coexistence of two TopIII $\alpha$ -RMI1 interfaces. To determine which interface is biologically relevant, we performed EM and single-particle analysis of negatively stained TopIII $\alpha$ -RMI complex sample used for growing crystals. b) Example of a negatively stained micrograph and individual particles marked with white squares. The scale bar corresponds to 50 nm. c) Reference-free class averages (top), reprojections of the 3D reconstruction (middle row) and reprojections of the crystal structure filtered at 30 Å resolution (bottom line) as matched by cross-correlation. d) The angular distribution for the TopIII $\alpha$ -RMI reconstruction mapped on a half sphere. The size of the spot is proportional to the number of raw images contributing to the class. (e) Fourier shell correlation (FSC) showing a resolution of 34 Å calculated using the 0.5 threshold criterion (dashed lines). f) Fitting of the two interfaces (ASU interface and biological interface) found in the crystal lattice in the calculated EM map. In the alternative orientation found in the ASU the orientation and location of RMI1 does not agree with the EM envelope demonstrating that the ASU interface is not the biological interface in solution. g) Different views of the fit between the crystal structure and the calculated EM map.

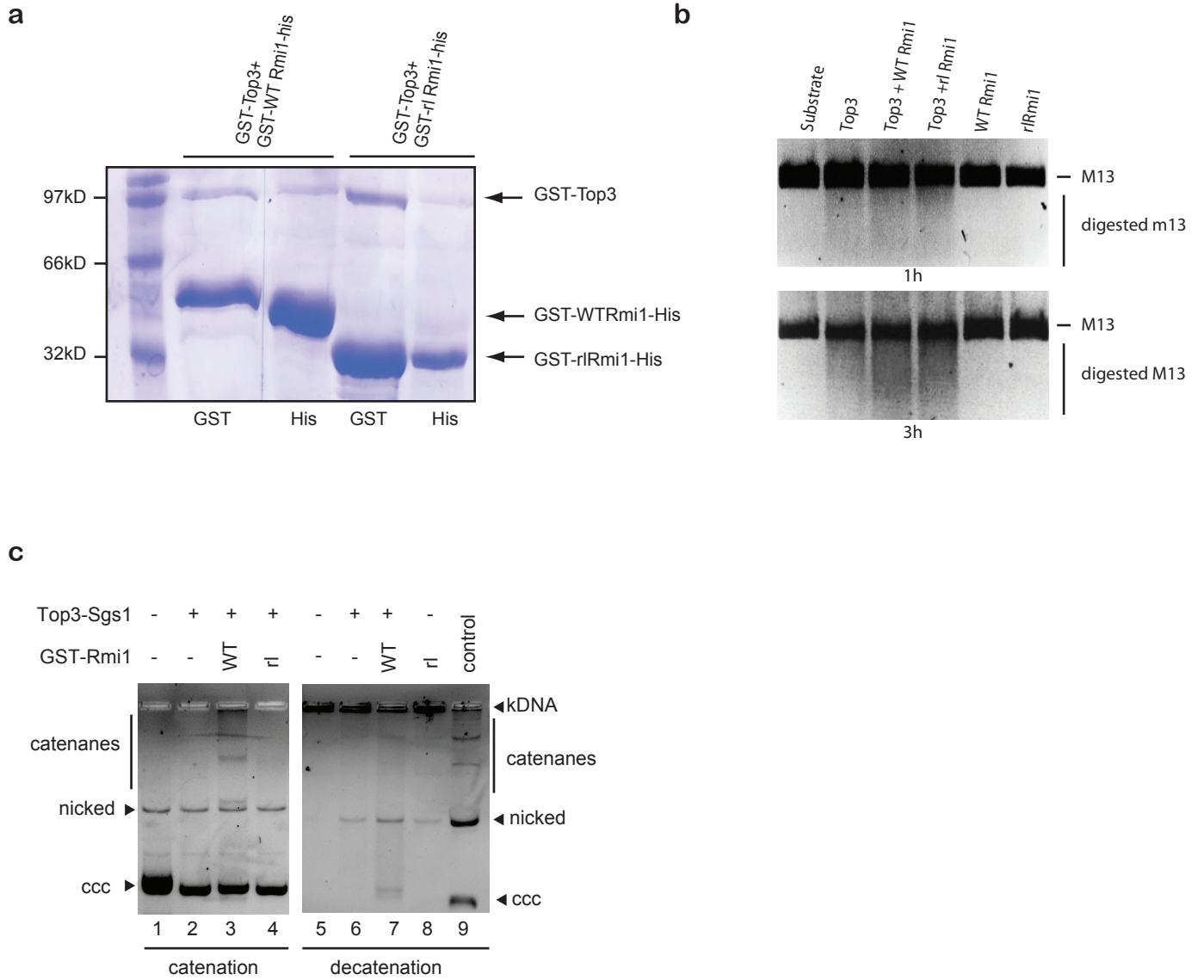


Supplementary fig. 4



#### Supplementary figure 4

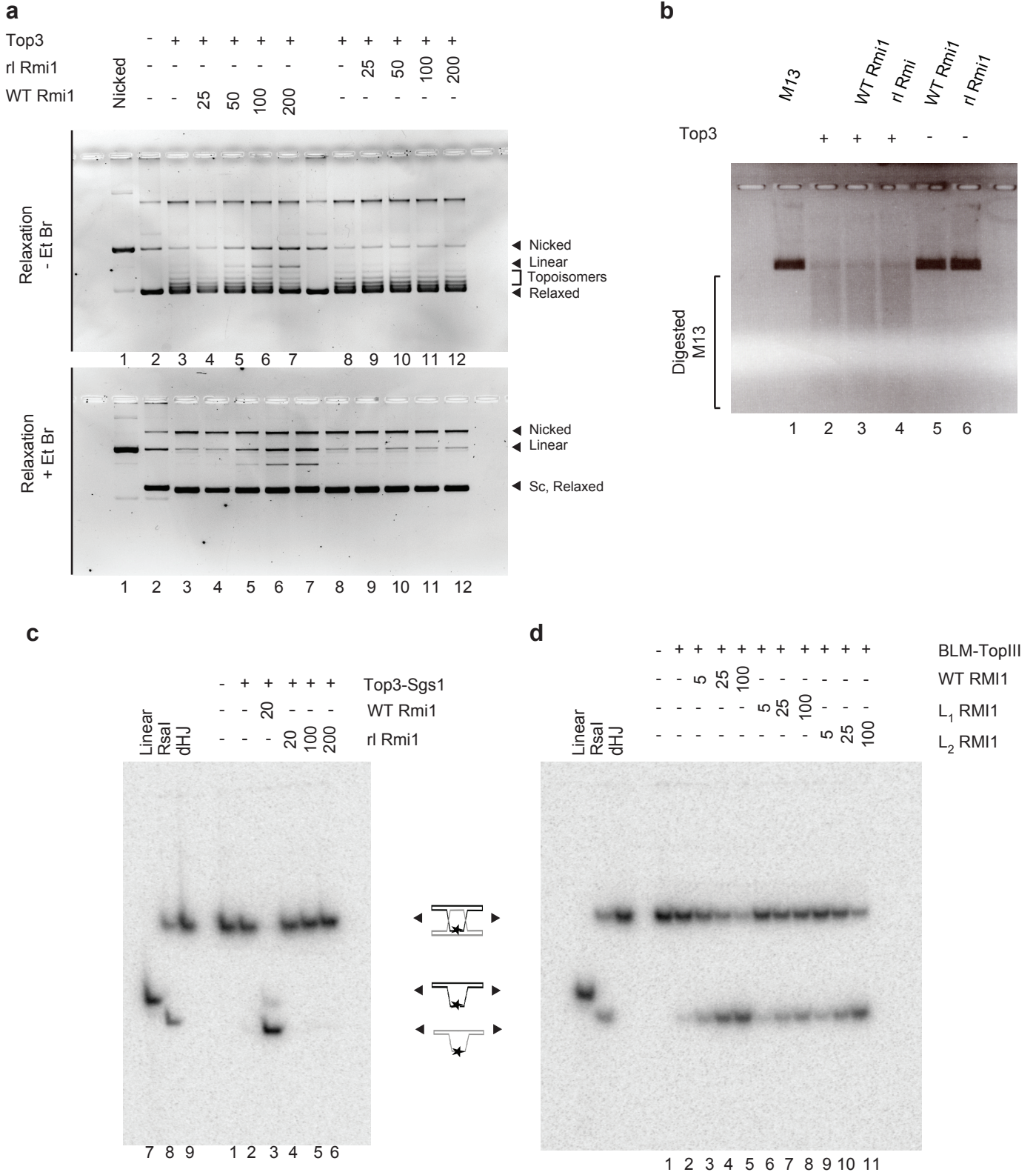
**Topology diagram and electronic density maps.** a) dHJs dissolution assay using the crystallized boundaries (TopIII $\alpha$ -RMI1)<sub>cb</sub> at the indicated concentrations, BLM 10 nM for 10 min incubation and 30 nM for 30 min incubation. *RsaI* Lane was used as a migration marker for the product of dHJ dissolution. The dissolution of dHJs is proportional to the (TopIII $\alpha$ -RMI1) concentration and is complete after 30 min incubation. This demonstrates that the crystallized complex is a minimal dissolvasome and defines the minimal domains belonging to a functional enzymatic core. b) Topology scheme of the crystallized complex represented as secondary structure elements with the same colour code as in Figure 1. Dashed lines represent disordered regions in the crystal. c) Crystal packing. One heterodimer is represented as surface (Green for TopIII $\alpha$  and red for RMI1) and corresponds to the biological unit. The close-up shows that the RMI1 decatenation loop is not involved in any crystal contacts. d,e) 2mFo-DFc omit maps contoured at 0.5 $\sigma$  and final refined models obtained in the Mg<sup>2+</sup> (d) and Ca<sup>2+</sup> (e) conditions (see Methods) represented as ribbons; TopIII $\alpha$  in green with RMI1 depicted in red.



Supplementary fig. 5

### Supplementary figure 5

a) Pull-down experiments; Top3 is GST N-terminally tagged and wild-type Rmi1 and rIRmi1, as used in relaxation and catenation assays, have GST N-Terminally and His C-terminally tags. Both proteins were co-expressed in High-Five cells. In the Ni<sup>2+</sup>-NTA pull-down, Top3 is still able to interact with the rIRmi1 mutant as indicated by the presence of a Top3 band. b) M13 digest in presence of Top3-WTRmi1 and Top3-rIRmi1 complexes. Analyses were performed after 1 h and 3 h digestion. The smear shows that the initial cleavage occurring in the first step of relaxation process is not impaired by the rIRmi1 construct. c) Catenation and decatenation assays using the yeast proteins. 100 ng of pUC19 (catenation) or kDNA (decatenation) were incubated with Top3 and Sgs1 alone (lane 2 and 6), with the addition of 200 nM of GST-WTRmi1 (lane 3 and 7) or 200nM of GST-rIRmi1 (lane 4 and 8). Although GST-WTRmi1 stimulates both the pUC19 catenation (lane 2 and 3) and kDNA decatenation (lane 6 and 7) activity of Top3-Sgs1, no stimulation was observed in the presence of GST-rIRmi1 (lane 4 and 8). kDNA decatenated in the presence of Topoisomerase II (Inspiralis) was used as a migration marker for nicked and circular covalently closed (ccc) decatenation products (lane 9).



Supplementary fig. 6

## Supplementary figure 6

**Uncropped gels from the main figure 4.** a) Uncropped gels corresponding to fig 4a .Yeast Top3 relaxation assay using pUC19 DNA to assess the effect of yeast Rmi1 wild-type (WT Rmi1) *versus* rIRmi1. b) Uncropped gels corresponding to fig 4c. Digest of single stranded M13 substrate with the different complexes. c) Uncropped gels corresponding to fig 4d. dHJs dissolution assay of a short synthetic dHJ junction, using the yeast Top3, Sgs1 and Rmi1. d) Uncropped gels corresponding to fig 4e. dHJs dissolution assay of a short synthetic dHJ junction using the human TopIII $\alpha$ , BLM and RMI1.